

# BlockEmulator: An Emulator Enabling to Test Blockchain Sharding Protocols

Huawei Huang , Senior Member, IEEE, Guang Ye, Qinde Chen, Zhaokang Yin, Xiaofei Luo, Jianru Lin, Taotao Li, Qinglin Yang , Zibin Zheng , Fellow, IEEE

**Abstract**—Numerous blockchain simulators have been proposed to allow researchers to simulate mainstream blockchains. However, we have not yet found a testbed that enables researchers to develop and evaluate their new consensus algorithms or new protocols for blockchain sharding systems. To fill this gap, we develop BlockEmulator, which is designed as an experimental platform, particularly for emulating blockchain sharding mechanisms. BlockEmulator adopts a lightweight blockchain architecture such that developers can only focus on implementing their new protocols or mechanisms. Using layered modules and useful programming interfaces offered by BlockEmulator, researchers can implement a new protocol with minimum effort. Through experiments, we test various functionalities of BlockEmulator in two steps. Firstly, we prove the correctness of the emulation results yielded by BlockEmulator by comparing the theoretical analysis with the observed experiment results. Secondly, other experimental results demonstrate that BlockEmulator can facilitate the measurement of a series of metrics, including throughput, transaction confirmation latency, cross-shard transaction ratio, the queuing size of transaction pools, workload distribution across blockchain shards, etc. We have made BlockEmulator open-source in Github.

**Index Terms**—Blockchain, Testbed, Consensus Protocol, Blockchain Sharding

## I. INTRODUCTION

Blockchain researchers need an experimental tool to verify the correctness or test the performance of their proposed protocols and algorithms. A handful of blockchain simulators have been proposed in the literature for different aims. For example, BLOCKBENCH [1] is designed for simulating and analyzing the performance of private blockchains. VIBES [2] enables blockchain simulation in large-scale network topologies and offers powerful visualization tools. SimBlock [3] is an event-driven simulator, which is suitable for studying the effect of block propagation in blockchain networks. Other simulators (e.g., Ganache [4], EthereumJS TestRPC [5], Parity Ethereum [6], the built-in emulator of Hyperledger Fabric [7], and Corda [8]) focus on simulating the fundamental functions of a blockchain such as smart contracts and transactions.

On the other hand, we find that the experiments of existing blockchain publications are mostly conducted through simu-

This work was partially supported by the National Key R&D Program of China (No. 2022YFB2702304), NSFC (No. 62272496, No. 62032025), and Fundamental Research Funds for the Central Universities, Sun Yat-sen University (No. 231gbj019).

All the authors are with Sun Yat-Sen University, China.

Corresponding author: Qinglin Yang, and Zibin Zheng, Email: {yangqlin6, zhengzb}@mail.sysu.edu.cn

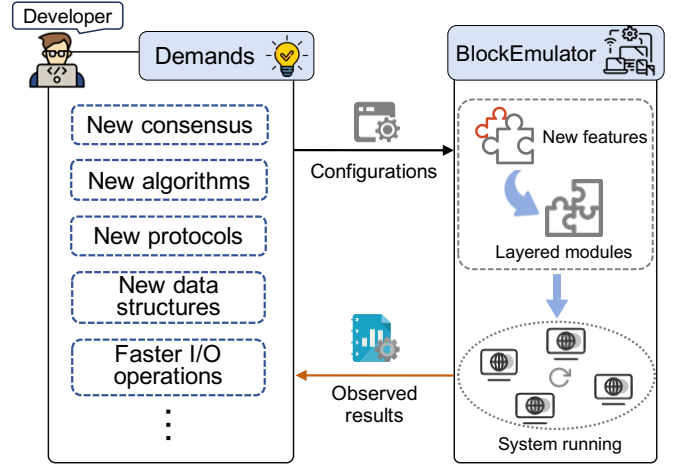


Fig. 1: The design principle of *BlockEmulator*.

lations. Their simulations must be implemented by building a new blockchain or using existing blockchains [9]–[11]. However, building a new blockchain from scratch requires a multitude of efforts, thus consuming a lot of time, not to mention designing new protocols on top of their new blockchain. Existing blockchains like Ethereum [12] have a vast codebase, thus making them unsuitable for designing new elements like consensus protocols. For instance, it’s challenging to design blockchain-sharding protocols on Ethereum, let alone re-designing other underlying layers such as the storage layer and data layer.

Given their merits, these existing simulators are not capable of supporting the demands of verifying new consensus protocols related to blockchain-sharding mechanisms. This is because a blockchain sharding system is complicated. It requires not only the design of intra-shard consensus but also the organization policy of shard committees, inter-shard consensus algorithms, cross-shard communication mechanisms, the security guarantee for blockchain shards, and the atomicity of executing cross-shard transactions, etc. Thus, the implementation of a blockchain-sharding mechanism is usually tailored in the context of designing a specific consensus algorithm for the sharded blockchain. When researchers shift their research focus, they have to implement a new blockchain sharding simulation as their experiment framework.

A better approach for blockchain researchers is to use a well-designed experiment platform that enables them to create new features of blockchain sharding with minimum

effort. To design an experimental tool that supports sharding mechanisms, it is necessary to determine the layered architecture of the sharded blockchain and develop the required components accordingly. Sufficient interfaces should be also provided in each component such that users can conveniently design new mechanisms without worrying about the code’s cross-layer operations. For example, S-Store [13] enables a dedicated data structure for the storage migration of shard data. If deploying a blockchain on S-Store, the focus would be mainly on implementing the underlying database interfaces of the blockchain and making minimal modifications to other layer data structures. Similarly, when deploying asynchronous BFT consensus algorithms on blockchain shards using Dispersedledger [14], users would only require modifying the consensus layer within each shard. In addition, to deploy account redistribution algorithms [15], users only need to modify partial communication mechanisms among shards in the consensus layer of Dispersedledger.

Implementing an experimental platform for blockchain sharding mechanisms involves multiple functionalities, including state management, cross-shard transactions, data availability, and inter-shard consensus. Therefore, a useful experimental tool of blockchain sharding should facilitate fast deployment and convenient support for testing various related metrics of a blockchain system. However, we have not yet found such an experimental tool in the literature. To fill this gap, we design a lightweight experimental platform, named *BlockEmulator*, which enables researchers to develop and test new blockchain sharding protocols. As depicted in Fig. 1, BlockEmulator only implements the core functions of a blockchain system, including node manager, consensus module, and on-chain transaction storage. For example, a client only has to configure the experimental parameters of BlockEmulator according to his/her design. After performing emulation, researchers can collect the experimental results from log files.

BlockEmulator also includes popular consensus protocols that can be utilized in sharded blockchains, such as Proof of Work (PoW) and Practical Byzantine Fault Tolerance (PBFT). In particular, BlockEmulator offers the system-level design and implementation of blockchain sharding mechanisms. The handling of cross-shard transactions implemented in BlockEmulator includes the following two representative solutions, i.e., *transaction relaying mechanism* proposed by Monoxide [16] and *BrokerChain* protocol [17].

The contributions of this paper are summarized as follows.

- To the best of our knowledge, BlockEmulator is the first available open-source experiment tool for evaluating blockchain sharding protocols and mechanisms.
- BlockEmulator provides a modular architecture design that enables researchers to quickly implement their new algorithms, protocols, and mechanisms. It also offers useful functions for researchers to help them collect experimental metrics.
- We designed experiments to show the correctness of BlockEmulator first. Other extensive experimental results demonstrate that BlockEmulator is capable of measuring various metrics of a sharded blockchain, including transaction throughput, transaction confirmation latency,

state of transaction pools, cross-shard transaction ratio, workload distribution across blockchain shards, etc.

The remainder of the paper is organized as follows. Section II is a background on PBFT, Sharding Mechanisms, and the Testing Environments of Existing Blockchain. Section III provides preliminaries and analysis of the cross-shard mechanism. Section IV presents the module design and framework of BlockEmulator with details. Section V conducts extensive experiments to validate the functional performance of BlockEmulator. Finally, Section VI concludes this work.

## II. BACKGROUND

In this Section, we introduce the background of the proposed BlockEmulator, including the Practical Byzantine Fault Tolerance (PBFT) consensus protocol, sharding mechanisms, and existing representative blockchain experiment tools.

### A. Practical Byzantine Fault Tolerance

PBFT [18] is a classic Byzantine fault-tolerant algorithm. Byzantine faults refer to those nodes that may send incorrect messages, tampered messages, or not send messages at all. PBFT guarantees that the system is still able to achieve consensus even when a certain number of Byzantine nodes exist in the system. This algorithm is widely used in mainstream blockchain systems such as consortium blockchains. For each consensus round, the main idea of PBFT is to select a primary node as the leader node, which is responsible for receiving and pre-processing requests from clients. When a proposal (e.g., a new block) is ready, the leader node broadcasts the proposal to other nodes. The other nodes decide whether to accept the proposal through voting. Once a certain number of nodes achieve a consensus, the proposal is confirmed. Then, this confirmed message proceeds to the next step of broadcasting. After going through the per-preparing, preparing, and committing phases, nodes achieve consensus and execute all transactions included in this confirmed proposal. Upon completing the execution of all transactions, the PBFT protocol sends a receipt message to clients. This round of PBFT finishes.

### B. Blockchain Sharding

Sharding technique divides a single blockchain into multiple parallel smaller blockchain shards to achieve scalability. Each blockchain shard is only responsible for maintaining the account state of a subset of transactions. Thus, the sharding mechanism can improve the throughput of the entire blockchain system.

Blockchain sharding can be classified into three categories, i.e., network sharding, transaction sharding, and state sharding. Among them, state sharding has become the research focus due to its low storage requirements [16], [17]. Following the static state sharding approach, if a proof-of-work (PoW) blockchain is segmented into  $S > 0$  shards, the blockchain’s performance has the potential to be scaled out by a factor of  $S$ . However, the computational power of the blockchain system will be distributed across all shards. Such the segmentation of consensus power reduces the security level to  $1/S$ . Malicious

nodes would make it easier to attack a specific shard with their consensus power. This is because there will always be a shard with computational power less than or equal to  $1/S$ , according to the pigeonhole principle [19]. Sacrificing a significant amount of security for higher throughput is not acceptable for a blockchain system. Therefore, the design of security mechanisms for blockchain sharding systems is crucial.

In blockchain systems that adopt the UTXO model, Monoxide [16] is a representative solution. The ‘‘Chu-ko-nu Mining’’ consensus proposed by Monoxide ensures that the security of the blockchain system does not decrease as the number of shards increases. All shards in Monoxide perform PoW consensus protocol simultaneously. Unlike the static state sharding algorithm, each shard’s PoW can be added to other shards’ local chains as long as it meets the mining difficulty. Through this approach, the effective computational power within each shard is amplified by a factor of  $S$  (i.e., the number of shards). This feature ensures the system’s security. Monoxide adopts the address partitioning policy by the address’s suffix, aiming to prevent malicious nodes from intentionally concentrating in one specific shard.

In state sharding that adopts the account/balance-based transaction model, the blockchain system can be described as a structure consisting of a final committee and several worker shards. The final committee is also called the *main* shard. In such cases, the blockchain system usually combines multiple mechanisms rather than relying on a single pure consensus mechanism. Committee members are periodically elected using more secure mechanisms like PoW to prevent Sybil attacks [20] and bribery attacks [21]. *Worker* shards generally employ high-throughput consensus mechanisms like PBFT for block generation to improve the system’s throughput. The main shard is responsible for various configurations and adjustments that benefit the performance of the blockchain. For example, the main shard makes periodic reconfiguration to the blockchain sharding system. The performance of the sharded blockchain system is mainly provided by the *worker* shards. While running, the blockchain sharding system goes to the next consecutive epoch when a specific running time expires or after a predefined number of blocks are generated. A reconfiguration phase will be executed before the next epoch begins.

### C. Representative Blockchain Experiment Tools

Through a thorough review of the literature, we have found the following representative simulators, emulators, or platforms that can be adopted as experiment tools for blockchain researchers.

- Ganache [4], formerly called TestRPC, is a blockchain emulator developed by Truffle Suite. It provides a local blockchain environment that allows developers to simulate Ethereum networks. Ganache supports features like smart contract development, transaction simulation, and account management.
- EthereumJS TestRPC [5] is a *Nod.js*-based emulator that provides a local Ethereum blockchain for testing and

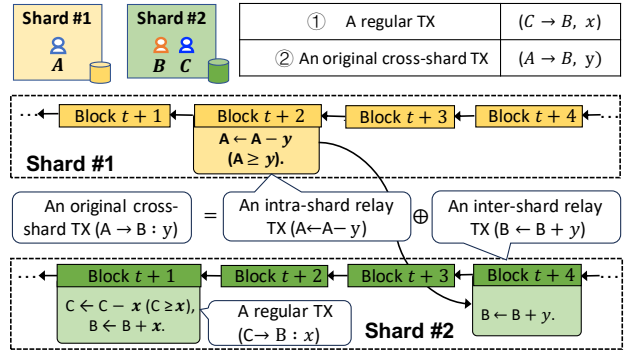


Fig. 2: The illustration of multiple types of transactions, including a regular transaction, an original cross-shard transaction, an intra-shard relay transaction, and an inter-shard relay transaction.

development purposes. It offers a lightweight and configurable environment for running test codes and deploying smart contracts.

- Parity Ethereum [6] provides a fully functional environment with mining capabilities, account management, and smart contract deployment. It enables developers to create a local private blockchain for testing Ethereum applications.
- Hyperledger Fabric [7] is a permissioned blockchain platform, which provides a built-in emulator for testing smart contracts and applications. It provides a local development environment that allows developers to simulate a blockchain network, create and interact with channels, deploy and invoke chain codes, and test consensus mechanisms.
- Corda [8] is a blockchain platform designed for enterprise, including a mock network feature that allows developers to emulate a Corda network for testing and development. The mock network provides a simulated environment to deploy and test Corda contracts, flows, and transactions.

Given the existing experiment tools, we can find that these efforts mainly focus on the functions of smart contracts and transaction executions. Nevertheless, we have not found a dedicated emulator that offers blockchain-sharding mechanisms and the handling of cross-shard transactions.

## III. PRELIMINARIES OF BLOCKCHAIN SHARDING

In this section, we elaborate on the preliminaries of blockchain sharding mechanisms, including the terminologies, concepts, and critical issues of blockchain sharding.

### A. Cross-Shard Transactions

As shown in Fig. 2, suppose that there are three accounts  $A$ ,  $B$ , and  $C$ , and two blockchain shards. Accounts  $B$  and  $C$  locate at Shard #2, while Account  $A$  locates at Shard #1. Thus, the transaction  $(C \rightarrow B : x)$  is called a *regular* TX, which will be handled only in Shard #2. In contrast, the transaction  $(A \rightarrow B : y)$  becomes a *cross-shard* TX.

TABLE I: Symbols defined for Transaction Types.

$\mathcal{U}$	The set of all inter-shard relay TXs
$\mathcal{V}$	The set of all intra-shard relay TXs
$\mathcal{W}$	The set of all TXs packed in historical blocks
$\mathcal{X}$	The set of all historical TXs submitted to TXpools by TX payers
$\mathcal{Y}$	The set of all historical cross-shard TXs
$\mathcal{Z}$	The set of all historical regular intra-shard TXs

Monoxide [16] divides an original cross-shard transaction ( $A \rightarrow B : y$ ) into an *intra-shard* relay transaction ( $A \leftarrow A - y$ ) and an *inter-shard* relay transaction ( $B \leftarrow B + y$ ), aiming to achieve the so-called *eventual atomicity* of a cross-shard transaction. The intra-shard relay transaction deducts the funds from the payer’s account in the source shard, while the inter-shard relay transaction deposits the funds into the payee’s account in the destination shard. These two relay transactions are connected through transaction-relaying messages.

While handling all transactions in each shard, miners select transactions from the local transaction pool (abbr. as TXpool) to generate a new block. These miners can interpret whether an original transaction in the block is a cross-shard transaction (abbr. as CTX) or an intra-shard regular transaction according to the locations of the payer and payee accounts. That is, the inter-shard relay transaction of the original CTX will be relayed to the payee’s shard (i.e., the destination shard) after the block is committed on the payer’s shard local chain. Once a consensus node receives an inter-shard relay transaction, it will check whether the related intra-shard relay transaction has been successfully included in the blockchain ledger. If the corresponding intra-shard relay transaction is on the chain, this consensus node adds the inter-shard relay transactions to its TXpool for future packaging.

As shown in Table I and Fig. 2, to better understand the correlations between inside-shard and cross-shard transactions in a sharded blockchain, we let  $\mathcal{U}, \mathcal{V}, \mathcal{W}, \mathcal{X}, \mathcal{Y}, \mathcal{Z}$  denote the set of inter-shard relay transactions, intra-shard relay transactions, transactions packed into all historical blocks, all historical transactions submitted to TXpools by TX payers, all historical cross-shard transactions, and all historical regular transactions, respectively. Note that, all those non-cross-shard transactions are the *regular transactions*, which can be handled easily by the local consensus within a particular shard. Meanwhile,  $|\mathcal{X}|$  represents the size of  $\mathcal{X}$ , and the same meaning applies to other symbols.

Based on the description aforementioned, we have

$$|\mathcal{Y}| = |\mathcal{U}| = |\mathcal{V}|. \quad (1)$$

A cross-shard transaction is divided into two relay transactions and will be included in two blocks eventually, we thus have the following equation.

$$\begin{cases} |\mathcal{Z}| + |\mathcal{Y}| = |\mathcal{X}|, \\ |\mathcal{Z}| + 2 \cdot |\mathcal{Y}| = |\mathcal{W}|. \end{cases} \quad (2)$$

With  $|\mathcal{Y}| = |\mathcal{W}| - |\mathcal{X}|$  increasing, the number of transactions packed in the blockchain will be significantly greater than the

processed transactions in practice. Thus, a sharding blockchain suffers from high latency and low throughput due to the cross-shard coordination.

### B. Shard Workload Balance

Monoxide [16] allocates accounts into designated shards based on these accounts’ suffixes. However, as demonstrated in [17], some accounts could be very active and thus result in unbalanced workloads across shards. Monoxide neither considers how to reduce the proportion of CTXs nor how to balance shard workloads.

To the best of our knowledge, we have found two representative algorithms that can achieve workload balance for blockchain shards, i.e., CLPA [15] and BrokerChain [17]. They are introduced as follows.

CLPA [15] is a dynamic account allocation algorithm that is different from the static policy defined in Monoxide [16]. It can balance the workloads across shards and reduce the number of cross-shard transactions, simultaneously. In [15], committee nodes need to be selected by PoW at the beginning of each epoch. The committee then listens to newly generated blocks from each shard and generates a graph of accounts according to these new blocks. In this graph, edges are the transactions enclosed in the blocks and vertexes are the accounts associated with these transactions. When an epoch expires, the committee runs CLPA, which then returns the account reallocation results. The account graph is updated each epoch so that the workload balance across shards can be achieved by invoking graph partition algorithms such as Metis or the community-aware graph partition algorithm.

Huang *et al.* [17] proposed the BrokerChain protocol, aiming to reduce the number of cross-shard TXs. BrokerChain selects some particular accounts as *broker accounts*, each of which is duplicated in multiple shards. A CTX is transferred into two intra-shard regular transactions in BrokerChain protocol. Those two regular TXs can be quickly handled in the payer’s and payee’s shards, respectively. The quantity of transferred tokens of the original CTX is *bridged* by one specific broker account. Note that, if the payer or payee of a CTX is a broker account, this CTX becomes a regular transaction essentially. That is why BrokerChain can reduce the number of CTXs significantly.

### C. The Composition of Sharding Consensus

In most blockchain sharding studies [15], [17], [22], [23], a sharding consensus protocols are composed of *worker* shards and *main* shard (i.e., the final committee). *Worker* shards are responsible for packaging blocks and achieving local consensus, while the *main* shard executes reconfiguration algorithms (e.g., CLPA [15]) and feeds back the results to the *worker* shards.

## IV. DESIGN AND IMPLEMENTATION OF BLOCKEMULATOR

In this section, we elaborate on the design and implementation of BlockEmulator.

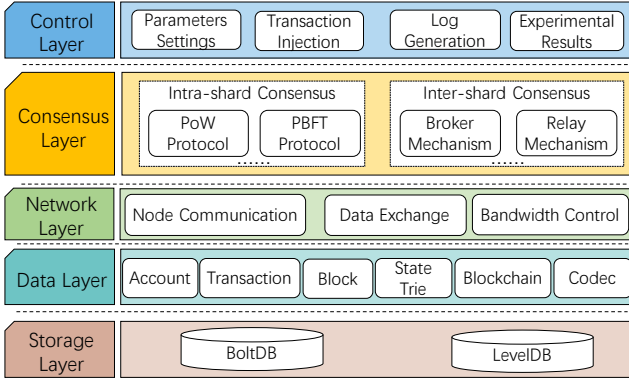


Fig. 3: The layered architecture of *BlockEmulator*.

#### A. Layered Architecture

Fig. 3 shows the overview of the layered architecture of *BlockEmulator*, which consists of *Storage Layer*, *Data Layer*, *Network Layer*, *Consensus Layer*, and *Control Layer*.

1) *Storage Layer*: The storage layer stores ledger data on the disk, including the generated blockchain data, log files generated when conducting experiments, etc. For instance, consensus nodes save the confirmed blocks, transactions, account states, and system logs. The storage layer’s functionality is implemented based on boltDB and levelDB. Particularly, we adopt the Merkle Patricia Tree (MPT) on top of levelDB, towards a more efficient I/O operation.

2) *Data Layer*: The data layer establishes fundamental structures of data within the system, including accounts, transactions, blocks, state trees, and nodes. The data layer interacts with the storage layer. When running *BlockEmulator*, new blocks are continually generated and encoded through the data layer. These new blocks trigger the modifications of state trees. These new tree nodes in state trees are encoded locally. The encoded blocks and account states can be stored in local files via invoking the interfaces of the storage layer. Furthermore, when an experiment is completed, the block data stored in files can be retrieved through the storage layer. The retrieved block data can be then decoded back into blocks by the data layer. Similarly, the retrieved root nodes of state trees in different blocks can be used to generate the state trees locally. This way enables researchers to access the generated blocks and account state trees. Thus, users can examine account states offline if they are curious about the correctness of transaction execution results yielded by *BlockEmulator*.

3) *Network Layer*: The network layer is designed to support the communication across consensus nodes deployed in diverse devices. An end-to-end packet transmission mechanism is implemented by TCP, aiming to exchange data among nodes. The data exchanged includes transactions, blocks, consensus messages, etc. We implement the TCP as a keep-alive connection manner to facilitate a substantial amount of message exchanges within the network. In this manner, the TCP connection between two nodes is initiated and closed only once during the overall emulation.

4) *Consensus Layer*: The consensus layer is responsible for enabling consensus nodes to reach an agreement on a new

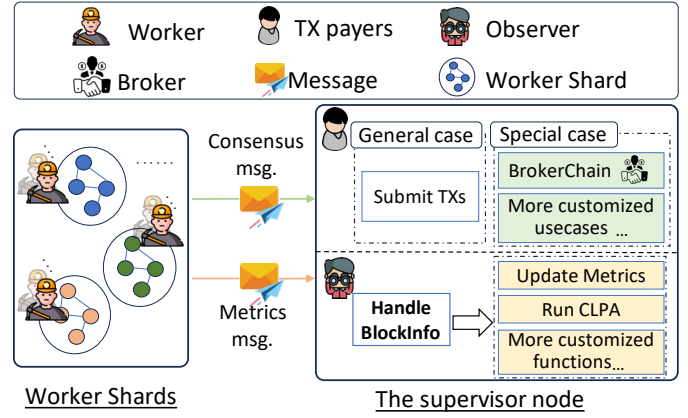


Fig. 4: Major roles of *BlockEmulator*, and the interactions between *worker shards* and the *supervisor node*.

block. In a sharded blockchain, nodes are running both the intra-shard and inter-shard consensus mechanisms. The intra-shard consensus mechanisms (like PoW and PBFT) ensure transaction consensus within a shard. The inter-shard mechanisms guarantee communication across shards. For example, to handle a CTX, the nodes located at the payer’s and payee’s shards should receive messages from other shards.

5) *Control Layer*: The control layer is in charge of the system execution. Before an experiment gets started, this layer needs to make preparations for configuring the experiment’s environment. Preparing the experiment’s environment includes initializing metric testing threads, starting listening to messages, determining the host of each consensus node, etc. When *BlockEmulator* is running, the control layer injects transactions to the transaction pools of shards at a predefined rate. The transactions injected into *BlockEmulator* can be retrieved from the historical transactions of any blockchain such as Ethereum. This layer also records the information of blocks generated by shards and the information includes not only the blocks themselves but also the necessary details of shards. When *BlockEmulator* finishes running an experiment, users can collect the experimental results from logs for scientific analysis.

#### B. Major Roles in *BlockEmulator*

As shown in Fig. 4, there are 2 types of nodes in *BlockEmulator*, i.e., *worker* nodes and *supervisor* nodes. A *worker* is responsible for packing transactions and generating blocks for the blockchain in each local shard. *Supervisor* nodes conduct global control behaviors, e.g., injecting transactions to shards, collecting committed blocks, and calculating system metrics. Note that, the number of required worker and supervisor nodes is determined by the blockchain network scale. The number of these two types of nodes can be configured flexibly according to the developer’s budget.

The behaviors of *supervisors* are executed concurrently. Different *supervisors* could commit different behaviors collaboratively. However, this multiple-supervisor implementation leads to the high complexity of the emulation system. To simplify *BlockEmulator*, we implement two roles, i.e., *TX*

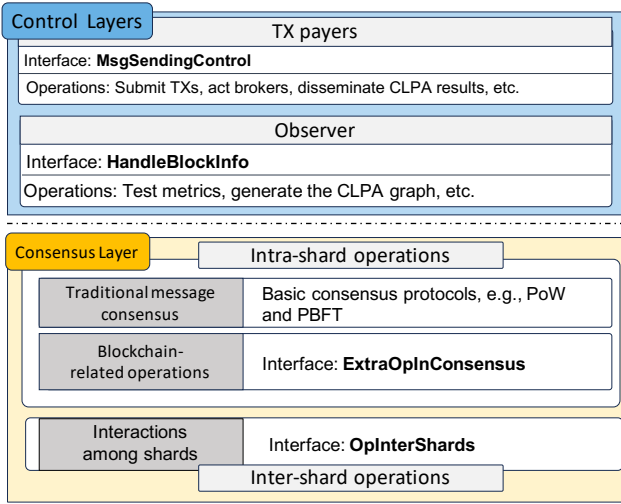


Fig. 5: The interfaces designed for Consensus Layer and Control Layer.

*payors* and *observer*. The first role takes on the responsibility of injecting transactions into the TXpool of each shard. As the second role, *observer* not only monitors the execution status of the blockchain system but also computes and records experimental outcomes.

Note that, in the real blockchains, there indeed are transaction payors who initiate transactions and observers who collect blocks. Accordingly, we consider these roles and add more features to them in our BlockEmulator. Both the *TX payors* and the *observer* can extend additional functionalities by invoking the interfaces presented in Section IV-C.

### C. Core Interface Modules

To alleviate the difficulty of secondary development based on our BlockEmulator, we not only implement some of the existing popular blockchain mechanisms as pre-installed modules but also design some application programming interfaces (APIs) to meet the compatibility among mechanisms. We show primary APIs in Fig. 5. We believe that users can easily implement their new mechanisms with a few codes using the following interfaces we provide.

1) *Interfaces in Consensus Layer*: In general, the consensus operations in a blockchain can be roughly classified into two categories: *traditional message consensus* and *blockchain-related operations*.

For example, PoW mechanism was born earlier than the blockchain as a mechanism to protect against spam emails originally [24]. In other words, PoW is a traditional message consensus and can be used in other distributed systems. However, in a blockchain environment, the PoW mechanism needs to do more operations related to blockchain, such as packing transactions, checking the correctness of all transactions enclosed in a block, and adding a new block to the blockchain.

Likewise, by incorporating blockchain-related operations, the traditional PBFT protocol can work in blockchain systems. Therefore, the details of these operations could be different

across blockchains. Users should focus on their needs when designing new mechanisms on top of BlockEmulator. The traditional message consensus part can be easily reused because it does not need to be modified in most scenarios.

According to the analysis above, we split *traditional message consensus* and *blockchain-related operations* in our implementations. We implement the interface **ExtraOpInConsensus** in the consensus layer for users to implement blockchain-related operations, including *mining* (occurs in the message generation phase), *checking* (occurs during consensus phase), and *confirming* (occurs in the phase after achieving the consensus).

In a sharded blockchain, a shard must interact with other shards. However, the traditional consensus such as PoW and PBFT do not provide such functionalities. To solve this problem while enabling secondary development, we enclose the **OpInterShards** as an interface, which can help users design the rules of message handling and broadcasting them among shards.

2) *Interfaces in Control Layer*: Recall that, in Section IV-B, the *supervisor* nodes play two roles (*TX payors* and *observer*) in the control layer. In practice, these two roles can be merged in only one *supervisor*, we thus implement one *supervisor* in the current version of BlockEmulator.

As illustrated in Fig. 4, we present two major interfaces of the *supervisor*. With these 2 interfaces, users can extend more features in *supervisor* according to their demands. We explain the functions of these two interfaces as follows.

Although the main duty of *TX payors* is to submit transactions, users can implement more useful application scenarios through the interface **MsgSendingControl**. For example, when the blockchain executes an account redistribution algorithm, *TX payors* can help to disseminate the up-to-date account distribution results to shards. In addition, in the scenario where the system emulates Brokerchain protocol [17], *TX payors* can execute the transaction-bridge function of *broker accounts*.

The second role *observer* is designed for analyzing the received block information from consensus nodes. With the dedicated interface **HandleBlockInfo**, the *observer* can make full use of the block information. For instance, when *BlockEmulator* emulates the account redistribution algorithm like CLPA [15], *observer* generates an account graph based on the historical blocks.

Users can also design how to collect their metrics using the interface **HandleBlockInfo**. After the computation of the specific metrics defined in this interface, these metrics are updated automatically when receiving a block. This customizable interface can facilitate the collection of experiment results.

### D. Particular Implementations

1) *Implementation of Account Redistribution*: In Section III-B, we have discussed CLPA algorithm [15]. The *Main* shard generates an account graph based on blocks collected from an epoch and runs CLPA on the graph when the current epoch expires.

We implement CLPA in *BlockEmulator* and separate the graph-related functions from the consensus layer. Users can

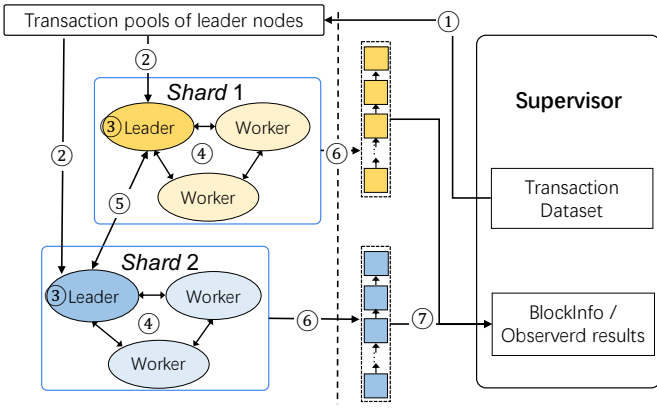


Fig. 6: The workflow of BlockEmulator. The seven steps when using BlockEmulator are explained as follows: ① : Supervisor first injects transactions. ② : Leaders load transactions from the pool. ③ : Leaders pack transactions into blocks. ④ : Consensus in shards. ⑤ : Interaction between shards. ⑥ : All nodes put blocks on the chain, update the state tree, and store data locally. ⑦ : Worker nodes send block information to the Supervisor.

thus invoke CLPA even in a non-blockchain environment. We also prune CLPA results to reduce their sizes. Accounts are called *dirty* ones if they need to migrate, and only these accounts will be added to the results of account redistribution.

To reduce the communication overhead among nodes, *BlockEmulator* adopts *observer* nodes as the members of the *Main* shard. The *supervisor* extends new functionalities for running CLPA and disseminating redistribution results to *worker* nodes, with **HandleBlockInfo** and **MsgSendingControl**, respectively. From a practical perspective, this approach does not influence the implementation of the sharding mechanism.

2) *Implementation of Account Migration*: When receiving the results of account redistribution, *worker* shards need to save the results and perform account migration.

*BlockEmulator* adopts a lock-based mechanism to implement the account migration. Once the leader of a *worker* shard receives a command of account redistribution, it should complete the current round of PBFT and suspend the PBFT consensus. Consequently, the leader determines which account's information should be sent to a new shard. The account information includes account states and the transactions associated with *dirty* accounts. This shard then unlocks its PBFT if the dirty account information is all received by destination shards. This shard then executes a consensus on the account migration. In other words, in one round of consensus, either account migration or transaction handling can occur at a time. Users can also replace the account migration mechanism according to their demands.

### E. Workflow of BlockEmulator

*BlockEmulator* works following the workflow depicted in Fig. 6, where we take PBFT as an illustrative intra-shard consensus.

- In step ①, users set up the configuration of the emulated blockchain. The system then generates a blockchain according to the configured parameters. Using PBFT protocol, the system designates a leader for each shard, after that all *worker* nodes will be initialized. The supervisor plays the role of *TX payers* and reads transactions from local files. It continuously injects transactions into the TXpool of each shard at a pre-defined static or dynamic rate.
- Then, in step ②, the leader node of each shard selects transactions based on specific rules such as prioritizing transactions by higher fees.
- After the leader node in a shard packages transactions to create a new block in step ③, the leader node initiates consensus such as PBFT.
- Subsequently, in step ④, the worker nodes in each shard achieve consensus. After that, the nodes will put the block on-chain, update the state tree, and store the block persistently in disks in step ⑥.
- If an operation requires information from other shards, nodes should communicate with them as shown in step ⑤. The contents of communications may include cross-shard transactions, account migrations, broker selections, etc.
- During the entire execution of the emulated blockchain, the supervisor also plays the role of *observer*. It monitors the operations and information of the whole blockchain, and updates metric data as shown in step ⑦.

The metric data and block information collected by the supervisor are stored in disks for experimental analysis.

## V. EXPERIMENTS AND ANALYSIS

To prove that *BlockEmulator* is useful and can produce correct emulation results, we show comprehensive measurements and tests in this section.

### A. Performance Metrics to Verify BlockEmulator

When analyzing the functional performance of *BlockEmulator*, we mainly focus on four metrics, including *transactions per second* (TPS) [25], *transaction confirmation latency* (TCL) [17], *cross-shard transaction Ratio* (CTX Ratio) [26], and *TXpool size*. A more detailed description of each metric is as follows.

- **TPS** is applied to measure the ability of transaction handling of a blockchain system. Note that, a cross-shard transaction is deemed confirmed if its *intra-shard* and *inter-shard* relay transactions are both on-chain. Thus, we count an intra-shard relay transaction or an inter-shard relay transaction as 0.5 in our calculation method for TPS.
- **TCL** is the interval counted from the timeslot when a transaction is proposed to the timeslot when this transaction is confirmed. In the context of blockchain, it refers to the time consumed between when a transaction is broadcasted to the network and when it is included in a block and confirmed by the network.
- **CTX Ratio** refers to the proportion of transactions whose payer and payee accounts are located in different shards

TABLE II: Symbols used in experimental settings.

$\Theta$	Size of a block
$\delta$	Interval between two blocks (second)
$\mathcal{R}$	The set of transactions handled
$N$	Number of shards
$t$	Time cost in the phase
$\phi$	The speed of transaction packing
$\mathbb{E}'(\text{TPS})$	TPS expectation for a single shard
$\mathbb{E}(\text{TPS})$	TPS expectation for the whole system

out of the total number of transactions submitted to TX-pools. A transaction requires less overhead for message propagation and storage if its payer and payee accounts are located in the same shard. A higher CTX Ratio might lead to longer latency and lower throughput.

- **TXpool size** stands for the length of the TXpool queue. It can not only reflect real-time changes in the TXpool but also indicate the transaction workload of each shard.

### B. Experimental Settings

In the following experiments, a block can maintain a maximum of 2,000 transactions. The interval between two blocks in each shard is set to 8 seconds. Each epoch lasts for 80 seconds. These settings allow users to analyze the system's performance in different epochs. The experiments are conducted on 10 resource-heterogeneous physical machines configured with the Ubuntu 20.04.6LTS operating system. The hardware configurations of those physical machines are 5 Xeon(R) W-2150B CPU and 64 GB RAM, 3 Inte(R) Core(TM) i7-9700F CPU and 64GB RAM, 1 Inte(R) Core(TM) i7-9700F CPU and 16 GB RAM, 1 AMD Ryzen 9 3900x 12 core CPU and 16 GB RAM. Moreover, multiple shards are deployed on each physical machine. Most modules of *BlockEmulator* are implemented using the Go language. Please find our open-source implementation from GitHub project <sup>1</sup>.

### C. Correctness of the Results Observed from BlockEmulator

To demonstrate the correctness of *BlockEmulator*, we conduct this group of experiments at a high scale. We evaluate the TPS versus different numbers of shards. We also set the total number of transactions to  $100,000 \times N$ , where  $N$  is the number of shards in each group of experiments. Therefore, the system runs for a sufficiently long time under different settings of  $N$ .

For a more detailed validation, we provide a special experiment setting. We generate transactions randomly to ensure their distribution across shards is balanced. We also control the transaction fees so that the priorities of transactions are equal in TXpools. The TXpool of each shard thus becomes a queue satisfying first-in-first-out (FIFO). To mitigate the impact of transaction injection, the nodes collect all transactions and put them into TXpools before the consensus starts. In addition, the system utilizes the *Relay* mechanism [16] to process cross-shard transactions and applies a static sharding algorithm.

Finally, we calculate the mathematical expectations of TPS in 3 phases and compare the experiment results obtained from BlockEmulator with the theoretical computation results.

1) *Mathematical Expectations in 3 Phases*: Each shard begins to handle inter-shard relay transactions until all the regular transactions and intra-shard relay transactions are handled in the TXpool. This is because the TXpool is a FIFO queue and all transactions have been collected before the system starts to run. With the settings depicted above, there are the following 3 phases, i.e., (Phase-1) the time before inter-shard relay transactions are handled, (Phase-2) the time when the inter-shard relay transactions are handled, and (Phase-3) the whole operation time while the system runs.

The relevant symbols and explanations are provided in Tab. II. The equation  $\mathbb{E}(\text{TPS}) = \mathbb{E}'(\text{TPS}) \times N$  holds due to the balanced workloads of all shards. We can derive from Eq.(1) that  $|\mathcal{U}| = |\mathcal{V}| = |\mathcal{Y}| = \frac{N-1}{N} \cdot |\mathcal{X}|$ ,  $|\mathcal{Z}| = \frac{1}{N} \cdot |\mathcal{X}|$ . We can also calculate the speed of transaction packing:  $\phi = \Theta \cdot N/\delta$ .

Then, let  $\mathbb{E}_1(\text{TPS})$ ,  $t_1$ ,  $\mathcal{R}_1$  and  $\mathcal{W}_1$  denote  $\mathbb{E}(\text{TPS})$ ,  $t$ ,  $\mathcal{R}$  and  $\mathcal{W}$  in Phase-1, respectively. Similar symbols apply to the other 2 phases. The mathematical expectations of TPS of these 3 phases are provided as follows.

- **Phase-1.** In this phase, the system packs both regular and intra-shard relay transactions into blocks, since inter-shard relay transactions are at the end of the TXpool queues. According to the  $|\mathcal{V}|$  and  $|\mathcal{Z}|$ , we can get  $|\mathcal{R}_1| = |\mathcal{V}|/2 + |\mathcal{Z}| = \frac{N+1}{2N} \cdot |\mathcal{X}|$ , and  $|\mathcal{W}_1| = |\mathcal{V}| + |\mathcal{Z}| = |\mathcal{X}|$ . The expectation time cost  $t_1$  can be calculated as dividing  $|\mathcal{W}_1|$  by the transaction packing speed  $\phi$ . Thus, we have  $t_1 = |\mathcal{W}_1|/\phi = \frac{\delta \cdot |\mathcal{X}|}{\Theta \cdot N}$ . Therefore, the TPS expectation for Phase-1 is expressed as:

$$\mathbb{E}_1(\text{TPS}) = |\mathcal{R}_1|/t_1 = \frac{\Theta \cdot (N+1)}{2\delta}. \quad (3)$$

- **Phase-2.** In this phase, the system handles the inter-shard relay transactions only. A block packs a number  $\Theta$  of transactions but the credit is only  $\Theta/2$ . Thus,  $\mathbb{E}_2(\text{TPS})$  can be calculated by dividing the speed of transaction packing by 2:

$$\mathbb{E}_2(\text{TPS}) = \phi/2 = \frac{\Theta \cdot N}{2\delta}. \quad (4)$$

- **Phase-3.** In the whole execution, the number of transactions the system packs is  $|\mathcal{W}_3| = |\mathcal{Z}| + |\mathcal{U}| + |\mathcal{V}| = \frac{2N-1}{N} \cdot |\mathcal{X}|$ . Here,  $t_3$  is the time cost by packing these  $|\mathcal{W}_3|$  transactions on the chain, and it can be calculated like that in Phase-1:  $t_3 = |\mathcal{W}_3|/\phi = \frac{\delta \cdot (2N-1) \cdot |\mathcal{X}|}{N^2 \cdot \Theta}$ . Therefore, the TPS expectation in Phase-3 is written as:

$$\begin{aligned} \mathbb{E}_3(\text{TPS}) &= |\mathcal{R}_3|/t_3 = |\mathcal{X}|/t_3 \\ &= \frac{N^2 \cdot \Theta}{2\delta}. \end{aligned} \quad (5)$$

2) *Experiment results and comparisons*: Fig.7 shows the piecewise TPS for each epoch when the number of shards varies. The two dashed lines in this figure refer to  $\mathbb{E}_1(\text{TPS})$  and  $\mathbb{E}_2(\text{TPS})$ , i.e., the TPS expectations for Phase-1 and Phase-2, respectively. In the six sub-figures, the curves of TPS decrease when the epoch shifts from Phase-1 to Phase-2. In addition,

<sup>1</sup><https://github.com/HuangLab-SYSU/block-emulator>

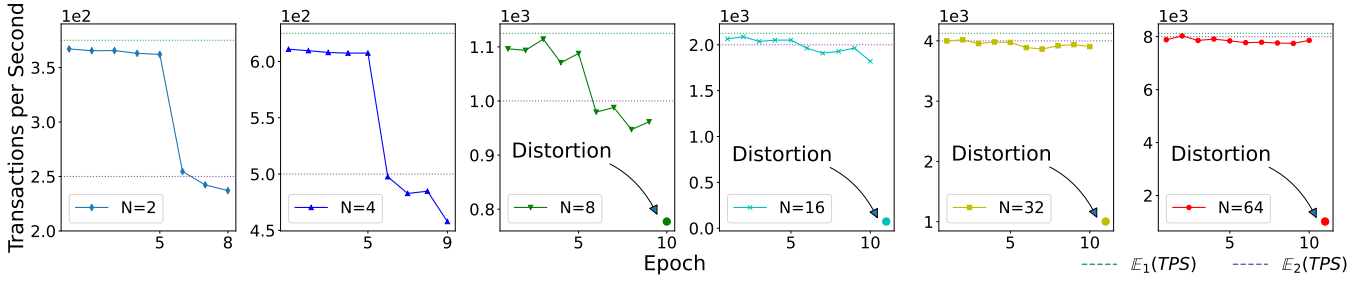


Fig. 7: Comparison of the theoretical results and experimental results in terms of TPS. The two horizontal dashed lines in each figure represent the  $\mathbb{E}_1(TPS)$  and  $\mathbb{E}_2(TPS)$  in the corresponding setting of shard numbers.

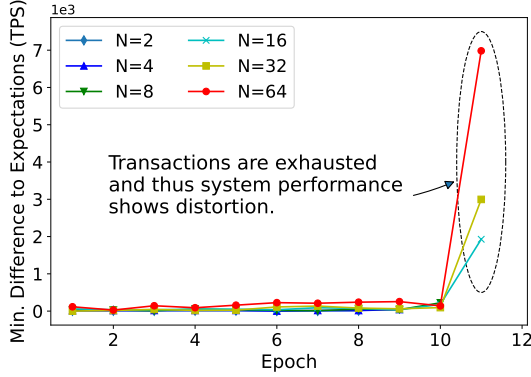


Fig. 8: The minimum differences calculated by  $\min(|obs(TPS) - \mathbb{E}_1(TPS)|, |obs(TPS) - \mathbb{E}_2(TPS)|)$ , which describes the performance gap between the observed performance and the theoretical expectations.

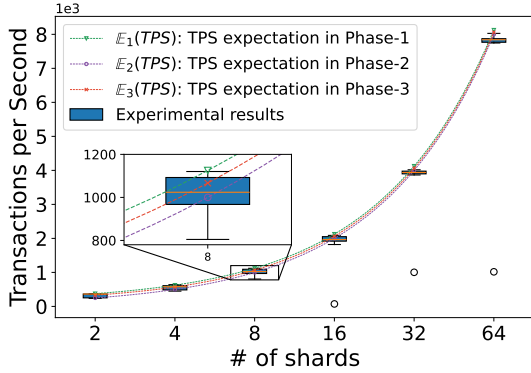


Fig. 9: Comparison of the theoretical expectations on TPS and experimental results in 3 phases.

except for the descent part, TPS curves stabilize around the two dashed lines corresponding to  $\mathbb{E}_1(TPS)$  and  $\mathbb{E}_2(TPS)$ . These findings confirm that the results of the experiments are as expected.

As the number of shards increases,  $\mathbb{E}_1(TPS)$  and  $\mathbb{E}_2(TPS)$  show a tendency to get closer to each other. Their gap narrows proportionally from  $1/2$  at  $N = 2$  to  $1/64$  at  $N = 64$ , although they always differ numerically by 125. The large  $N$  also leads to the severe disturbances of TPS. The decline from Phase-1 to Phase-2 is thus less clearly reflected when  $N = 64$ . The

TPS drops significantly at the last epoch in each experiment because the TXpools are exhausted at that time. Thus, the performance in the final epoch shows distortion.

Fig.8 illustrates the minimum differences between the observed TPS of each epoch and the expected TPS when the number of shards varies. The y-axis value (min. **Difference to Expectations**) describes the gap between the observed performance and the theoretical expectations. Fig.8 displays a consistently low minimal difference (within 250 txs/s) except for the last epoch of experiments, in which the performance distortion is caused by the exhausted transactions in shards. The results shown in this figure indicate that the observed experimental results are close to the theoretical expectation.

Fig. 9 depicts the experimental TPS of each epoch and the phase-wise TPS expectations. As shown in this figure, the TPS mean points essentially fall on the curve represented by  $\mathbb{E}_3(TPS)$ .

Both Fig. 8 and Fig. 9 demonstrate that neither the correctness nor the stability of the system is greatly affected when the number of shards increases.

#### D. Various Metrics are Supported to Measure

To show adequate performance testing functionalities of *BlockEmulator*, we conduct another group of experiments, in which approximately 1.6 million historical transactions of Ethereum [27] were adopted as the dataset. The number of shards is set to 32 and the number of nodes in each shard is set to 4. In other words, we run 128 nodes in our physical machines. In addition, we fix the transaction injection rate with 4,000 txs/s by default and increase it by 4,000 txs/s each the next epoch.

To reveal the features of supporting secondary development, we also implement some state-of-the-art mechanisms in our *BlockEmulator* and compare them using different metrics. The mechanisms we have implemented are introduced as follows.

- **Relay+Static.** The system handles cross-shard transactions with *transaction relay mechanism* [16]. The account states are divided into different shards by a static sharding method.
- **Relay+CLPA.** The cross-shard transaction handling method is *transaction relay mechanism*. The account states are redistributed using CLPA [15], which is a dynamic sharding algorithm.

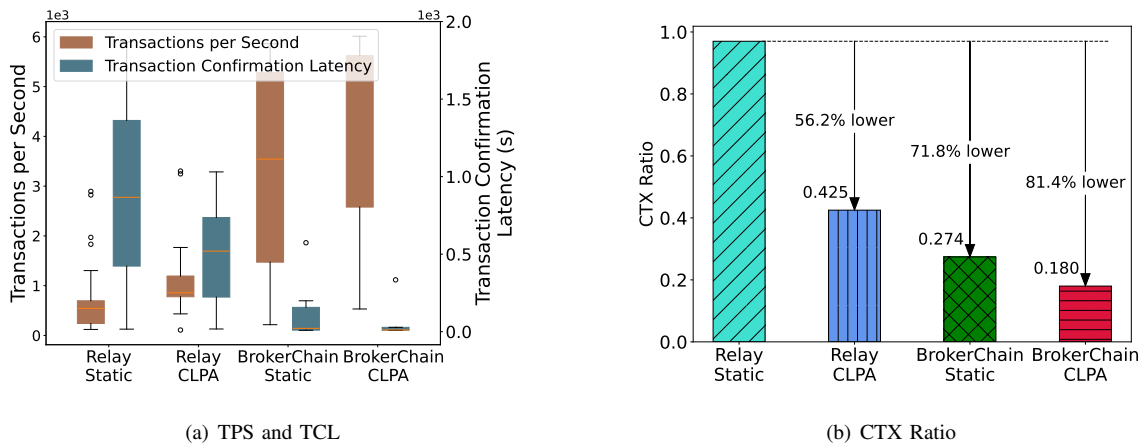


Fig. 10: Evaluation on TPS, TCL, and CTX Ratio while invoking 4 mechanisms, i.e., Relay+Static, Relay+CLPA, BrokerChain+Static, and BrokerChain+CLPA.

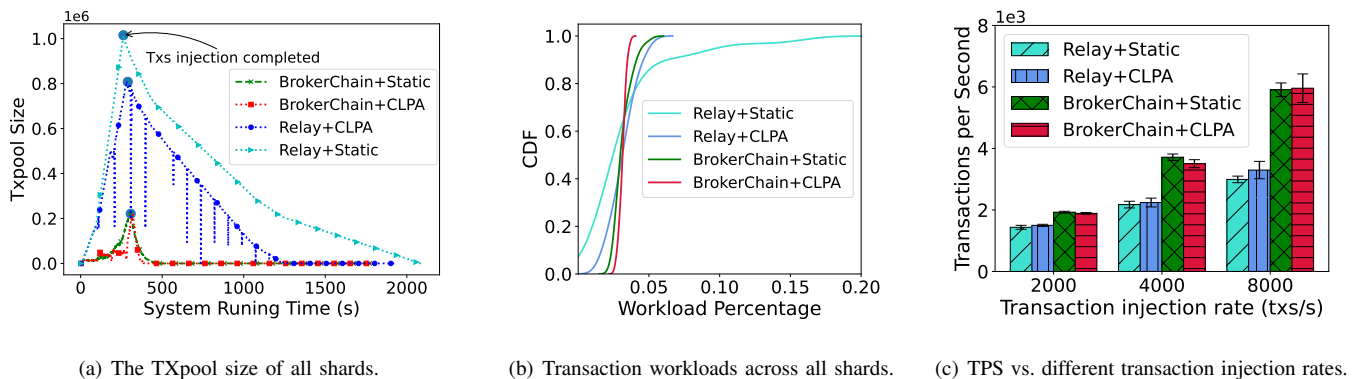


Fig. 11: Evaluation on time-varying TXpool size, workloads, and TPS vs. different Tx injection rates.

- **BrokerChain+Static.** BrokerChain protocol [17] is adopted to handle cross-shard transactions. The account states are sharded statically.
- **BrokerChain+CLPA.** This mechanism integrates the solutions of broker accounts and CLPA.

We select the top 10 accounts that transfer the most transactions as broker accounts in our experiments. The transactions in which these broker accounts are involved have a proportion of 80% of total transactions. With these well-selected broker accounts, the BrokerChain-related mechanisms thus get a better performance. We use an offline-version CLPA algorithm on partial data and find that the CTX Ratio is reduced by about 55%. Therefore, we expect that *BrokerChain+Static* will outperform *Relay+CLPA*, and *BrokerChain+CLPA* will show better performance than *BrokerChain+Static*.

As depicted in Fig. 10(a), *BrokerChain+Static* outperforms *Relay+CLPA*, and both of them perform better than *Relay+Static* in terms of TPS and TCL. The results of this group of experiments perfectly match what we predicted in the previous paragraph.

Interestingly, *BrokerChain+CLPA* does not show a dominating advantage than *BrokerChain+Static*. One possible reason is that the *CLPA* algorithm requires a reconfiguration stage for account migration, resulting in additional time consumption.

Another reason can be inferred from Fig. 10(b), in which it implies that *Relay+CLPA* has a much lower CTX ratio than *Relay+Static*. However, *BrokerChain+CLPA* has a slightly lower CTX ratio than *BrokerChain+Static*. This means that *BrokerChain* mechanism has already significantly reduced the CTX Ratio, and the impact of running *CLPA* is thus not apparent.

Fig. 11(a) shows that the accumulative size of TX-pools varies over time. Note that, in mechanisms *BrokerChain+CLPA* and *Relay+CLPA*, TXpool size suddenly descends and rises at some timeslots. This is because the transaction mitigation operations in *CLPA*. In addition, the TXpool size performance of both *BrokerChain+Static* and *BrokerChain+CLPA* increases slowly but declines fast. This observation indicates that these two mechanisms yield higher TPS and fewer accumulated transactions in TXpools compared to the other two mechanisms.

To further explore why *BrokerChain+CLPA* and *BrokerChain+Static* perform better in Fig. 11(a), we evaluate the workload distribution across shards. The observed results are shown in Fig. 11(b). The workload of each shard is calculated by summing up the packed transactions in all committed blocks within the shard. *BrokerChain+CLPA* shows the most balanced workloads because its CDF curve rises rapidly. This

observation indicates a high density of workload percentages, which suggests balanced workloads across shards. The CDF curve of *Relay+Static* grows slowly, while the CDFs of the other 3 mechanisms reach 1.0 fast. This observation shows that both *CLPA* and *BrokerChain* are effective when balancing workloads.

From Fig. 11(a), we find that the curves of *Relay+CLPA* and *Relay+Static* are close for the first 200 seconds. The curves of *BrokerChain+CLPA* and *BrokerChain+Static* show almost the same. These observations are interesting. Thus, we conducted another experiment to find some clues. This group of experiments runs for 1000 seconds. We record TPS every epoch (i.e., 80 seconds). To get adequate experimental data, we use about 8 million historical transactions collected from Ethereum [27].

Fig. 11(c) demonstrates the TPS of the 4 mechanisms at different transaction injection rates. Surprisingly, *CLPA* has few or negative effects while integrating with *Relay* and *Brokerchain* mechanisms. This is because *CLPA* improves TPS by moving transactions from the overloaded shards to the underloaded ones. However, there is almost no overloaded shard when the transaction injection rate is low. Similarly, there is almost no underloaded shard when the transaction injection rate is high. In addition, the reconfiguration time consumed by *CLPA* also leads to degradation of performance. Therefore, *CLPA* performs better if the transaction injection rate is low and TXpools are full. In Fig. 11(a), *CLPA* outperforms when transaction injection stops. This observation confirms our explanation aforementioned.

Finally, when the transaction injection rates are relatively low, the TPS of *BrokerChain+CLPA* and *BrokerChain+Static* are pretty close to the injection rates. This is because *BrokerChain* can shift a cross-shard transaction to a regular transaction if its payer or payee is a broker account. The proper broker accounts we selected for experiments help these two *BrokerChain*-related mechanisms work well.

## VI. CONCLUSION

BlockEmulator is designed as a testbed for blockchain researchers. It not only supports some basic operations in existing blockchains but also offers powerful programming interfaces for evaluating new blockchain protocols or consensus algorithms. In particular, it enables researchers to develop and evaluate new blockchain-sharding mechanisms. To verify the correctness of experiment data yielded by BlockEmulator, we conduct experiments to compare the observed performance with the theoretical calculation results. Other experiments prove that BlockEmulator supports meaningful performance testing in terms of typical metrics in a blockchain sharding system, including TPS, transaction confirmation latency, cross-shard transaction ratio, and the queuing length of transaction pools. We wish BlockEmulator could bring convenience to blockchain researchers when they need to design and test new mechanisms.

## ACKNOWLEDGEMENTS

We appreciate all the previous great efforts made by the students who graduated from HuangLab such as Xiaowen

Peng, Jianzhou Zhan, Shenyang Zhang, Canlin Li, and other team members who are not shown in the author list including Taotao Li, Yue Lin, Miaoyong Xu, Junhao Wu, Yetong Zhao, and Jian Zheng.

## REFERENCES

- [1] T. T. A. Dinh, J. Wang, G. Chen, R. Liu, B. C. Ooi, and K.-L. Tan, "Blockbench: A framework for analyzing private blockchains," in *Proc. of the 2017 ACM international conference on management of data*, 2017, pp. 1085–1100.
- [2] L. Stoykov, K. Zhang, and H.-A. Jacobsen, "Vibes: fast blockchain simulations for large-scale peer-to-peer networks," in *Proc. of the 18th ACM/FIP/USENIX Middleware Conference: Posters and Demos*, 2017, pp. 19–20.
- [3] Y. Aoki, K. Otsuki, T. Kaneko, R. Banno, and K. Shudo, "Simblock: A blockchain network simulator," in *Proc. of IEEE Conference on Computer Communications Workshops (INFOCOM WKSHPs)*. IEEE, 2019, pp. 325–329.
- [4] D. Mohanty and D. Mohanty, "Deploying smart contracts," *Ethereum for Architects and Developers: With Case Studies and Code Samples in Solidity*, pp. 105–138, 2018.
- [5] N. Prusty, *Building blockchain projects*. Packt Publishing Ltd, 2017.
- [6] OpenEthereum, "The Fastest and most Advanced Ethereum Client." <https://github.com/openethereum/parity-ethereum>, Retrieved: May 23, 2023.
- [7] E. Androulaki, A. Barger, V. Bortnikov, C. Cachin, K. Christidis, A. De Caro, D. Enyeart, C. Ferris, G. Laventman, Y. Manevich, et al., "Hyperledger fabric: a distributed operating system for permissioned blockchains," in *Proc. of the thirteenth EuroSys conference (EuroSys)*, 2018, pp. 1–15.
- [8] R. G. Brown, "The corda platform: An introduction," *Retrieved*, vol. 27, p. 2018, 2018.
- [9] M. Li, Y. Lin, J. Zhang, and W. Wang, "CoChain: High Concurrency Blockchain Sharding via Consensus on Consensus," in *IEEE INFOCOM 2023-IEEE Conference on Computer Communications*. IEEE, 2023, pp. 1–10.
- [10] M. Li, W. Wang, and J. Zhang, "LB-Chain: Load-Balanced and Low-Latency Blockchain Sharding via Account Migration," *IEEE Transactions on Parallel and Distributed Systems*, 2023.
- [11] Z. Hong, S. Guo, E. Zhou, W. Chen, H. Huang, and A. Zomaya, "GridB: Scaling Blockchain Database via Sharding and Off-Chain Cross-Shard Mechanism," *Proceedings of the VLDB Endowment*, vol. 16, no. 7, pp. 1685–1698, 2023.
- [12] G. Wood et al., "Ethereum: A secure decentralised generalised transaction ledger," *Ethereum project yellow paper*, vol. 151, no. 2014, pp. 1–32, 2014.
- [13] X. Qi, "S-Store: A Scalable Data Store towards Permissioned Blockchain Sharding," in *Proc. of IEEE Conference on Computer Communications (INFOCOM)*. IEEE, 2022, pp. 1978–1987.
- [14] L. Yang, S. J. Park, M. Alizadeh, S. Kannan, and D. Tse, "Disperse-dLedger: High-Throughput Byzantine Consensus on Variable Bandwidth Networks," in *Proc. of 19th USENIX Symposium on Networked Systems Design and Implementation*, 2022, pp. 493–512.
- [15] C. Li, H. Huang, Y. Zhao, X. Peng, R. Yang, Z. Zheng, and S. Guo, "Achieving Scalability and Load Balance across Blockchain Shards for State Sharding," in *Proc. of 2022 41st International Symposium on Reliable Distributed Systems (SRDS)*. IEEE, 2022, pp. 284–294.
- [16] J. Wang and H. Wang, "Monoxide: Scale out blockchains with asynchronous consensus zones," in *Proc. of 20th USENIX Symposium on Networked Systems Design and Implementation*, vol. 2019, 2019, pp. 95–112.
- [17] H. Huang, X. Peng, J. Zhan, S. Zhang, Y. Lin, Z. Zheng, and S. Guo, "Brokerchain: A cross-shard blockchain protocol for account/balance-based state sharding," in *Proc. of IEEE Conference on Computer Communications (INFOCOM)*, 2022, pp. 1968–1977.
- [18] M. Castro, B. Liskov, et al., "Practical byzantine fault tolerance," in *OsDI*, vol. 99, no. 1999, 1999, pp. 173–186.
- [19] W. A. Trybulec, "Pigeon hole principle," *Journal of Formalized Mathematics*, vol. 2, no. 199, p. 0, 1990.
- [20] S. Zhang and J.-H. Lee, "Double-spending with a sybil attack in the bitcoin decentralized network," *IEEE transactions on Industrial Informatics*, vol. 15, no. 10, pp. 5715–5722, 2019.

- [21] S. Gao, Z. Li, Z. Peng, and B. Xiao, "Power adjusting and bribery racing: Novel mining attacks in the bitcoin system," in *Proc. of the 2019 ACM SIGSAC Conference on Computer and Communications Security*, 2019, pp. 833–850.
- [22] L. Luu, V. Narayanan, C. Zheng, K. Baweja, S. Gilbert, and P. Saxena, "A secure sharding protocol for open blockchains," in *Proc. of the 2016 ACM SIGSAC conference on computer and communications security*, 2016, pp. 17–30.
- [23] M. Zamani, M. Movahedi, and M. Raykova, "Rapidchain: Scaling blockchain via full sharding," in *Proc. of the 2018 ACM SIGSAC conference on computer and communications security*, 2018, pp. 931–948.
- [24] C. Dwork, M. Naor, and H. Wee, "Pebbling and proofs of work," in *Advances in Cryptology—CRYPTO 2005: 25th Annual International Cryptology Conference, Santa Barbara, California, USA, August 14–18, 2005. Proceedings 25*. Springer, 2005, pp. 37–54.
- [25] S. King and S. Nadal, "Ppcoin: Peer-to-peer crypto-currency with proof-of-stake," *self-published paper*, August, vol. 19, no. 1, 2012.
- [26] Y. Zhang, S. Pan, and J. Yu, "Txallo: Dynamic transaction allocation in sharded blockchain systems," in *Proc. of IEEE 39th International Conference on Data Engineering (ICDE)*. IEEE, 2023, pp. 721–733.
- [27] P. Zheng, Z. Zheng, J. Wu, and H.-N. Dai, "XBlock-ETH: Extracting and exploring blockchain data from Ethereum," *IEEE Open J. Comput. Soc.*, vol. 1, pp. 95–106, May 2020.



**Zhaokang Yin** is currently a student pursuing his master's degree at the School of Software Engineering, Sun Yat-Sen University. His research interests mainly include Blockchain.



**Xiaofei Luo** is currently a postdoctoral researcher at Sun Yat-sen University. He received his Ph.D. degree in Computer Science and Engineering from the University of Aizu in March 2023. His current research interests include blockchain, payment channel networks, and reinforcement learning. His research has been published in IEEE JSAC and other well-known international journals and conferences.



**Huawei Huang** (SM'22) received his Ph.D. in Computer Science and Engineering from the University of Aizu, Japan. He is an associate professor at the School of Software Engineering, Sun Yat-Sun University, China. His research interests mainly include blockchain systems. He has served as a guest editor for multiple special issues on blockchain at IEEE JSAC, OJ-CS, and IET Blockchain. He also served as a TPC chair for a number of blockchain conferences, workshops, and symposiums.



**Lin Jianru** is a research scientist engineer of HuangLab (a blockchain laboratory at Sun Yat-sen University). He has rich experience in the design and implementation of decentralized systems, smart contract languages, and virtual machines. He is the translator of the Chinese edition of *Designing for Scalability with Erlang/OTP*.



**Guang Ye** is currently a student pursuing his master's degree at the School of Software Engineering, Sun Yat-Sen University. His research interests mainly include Blockchain.



**Taotao Li** received the Ph.D. degree in cyber security from the Institute of Information Engineering, Chinese Academy of Sciences and University of Chinese Academy of Sciences, China, in 2022. He is currently a postdoc with the School of Software Engineering, Sun Yat-Sen University, Zhuhai, China. His main research interests include blockchain, Web3, and applied cryptography.



**Qinde Chen** is a Ph.D. student at the School of Software Engineering, Sun Yat-sen University. His research interests mainly include blockchain.



**Qinglin Yang** received his M.S. degree in computing mechanism from College of Civil Engineering, Kunming University of Science and Technology in 2017, and a Ph.D. degree from the University of Aizu, Japan in computer science and engineering and 2021. He is a research fellow with the School of Intelligent System Engineering, Sun Yat-sen University. His research interests include edge computing, federated learning, and Blockchain.



**Zibin Zheng** (SM'16-F'23) received a Ph.D. degree from the Chinese University of Hong Kong, Hong Kong, in 2012. He is a Professor at the School of Software Engineering, Sun Yat-Sen University, China. His current research interests include service computing, blockchain, and cloud computing. Prof. Zheng was a recipient of the Outstanding Ph.D. Dissertation Award of the Chinese University of Hong Kong in 2012, the ACM SIGSOFT Distinguished Paper Award at ICSE in 2010, the Best Student Paper Award at ICWS2010, and the IBM Ph.D. Fellowship

Award in 2010. He served as a PC member for IEEE CLOUD, ICWS, SCC, ICSOC, and SOSE.